The Role of Chaos in Barred Galaxies

G. Contopoulos and N. Voglis

Department of Astronomy, University of Athens Panepistimiopolis, GR -157 84 Athens, Greece

Abstract. Ordered orbits in barred galaxies appear along the bar and between the $-4/1$ and $-2/1$ resonances of the outer spiral. Chaotic orbits appear mainly near corotation. Such orbits support the bar and the spiral for long times and they are important for self-consistency. There are three main mechanisms for transition from order to chaos: (a) infinite bifurcations, (b) infinite gaps, and (c) infinite spirals. The Lyapunov characteristic number is zero for ordered orbits and positive for chaotic orbits. But much more information is provided by the distribution of the stretching numbers (one-period Lyapunov characteristic numbers). The spectrum of stretching numbers is invariant with respect to initial conditions in a connected chaotic domain. We provide examples of such spectra for 2-D maps, plane galactic orbits, 2-D dissipative systems, 3-D systems (represented by 4-D maps), and systems depending periodically on the time.

1. Ordered and Chaotic Orbits

Barred galaxies contain both ordered and chaotic orbits. The ordered orbits are either periodic (Figure 1), or quasi-periodic (Figure 2), i.e. orbits trapped around some periodic orbits. Most orbits well inside corotation are ordered. They are trapped around the main families of periodic orbits, namely the central family (or family x_1), and the 4/1 family. These two types of orbits have different topology, but both are elongated along the bar. Thus both types support the bar.

There are also other types of stable periodic orbits, like the 3/1 and 1/1 orbits (Contopoulos & Grosbol 1989), that may play an important role in some bar models.

In a bar potential beyond corotation, up to the outer Lindblad resonance, most orbits are perpendicular to the bar (Contopoulos 1980), and this is one of the main reasons why bars cannot be self-consistent outside corotation. The other reason is that most orbits near corotation are chaotic. Thus bars end near corotation, or somewhat inside it (Contopoulos 1980). This conclusion is now generally accepted.

Let us assume further that beyond corotation we have a spiral rotating with the same angular velocity as the bar. Such a model is represented by a time
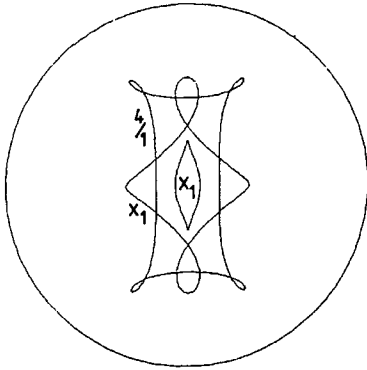
Figure 1. Periodic orbits of the families x_1 and 4/1 in the Florida galactic model (Contopoulos et al. 1989). The circle marks corotation.
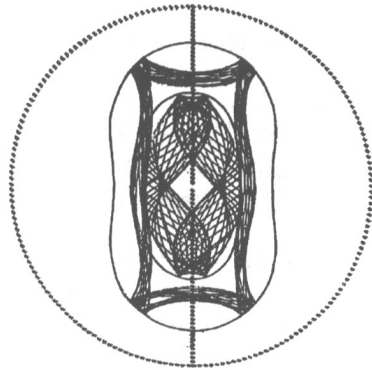
Figure 2. Two quasiperiodic orbits in the model of Figure 1, trapped around x_1 and 4/1. The almost oval curves surrounding the two orbits are the corresponding curves of zero velocity.

independent Hamiltonian of the form

$$H \equiv \frac{1}{2}v^2 + V_o + \varepsilon V_1 - \Omega_s J = h, \qquad (1)$$

where v is the velocity in the frame rotating with angular velocity Ω_s, V_o is the axisymmetric background potential, εV_1 is the bar-spiral potential, J is the angular momentum of a star and h is the numerical value of the Hamiltonian, i.e. the Jacobi constant.

In such a model there are ordered orbits supporting the spiral outside corotation, mainly between the $-4/1$ resonance and the outer Lindblad resonance (OLR) (Figure 3).

However closer to corotation there are many chaotic orbits (Figures 4, 5). Figure 4 represents a chaotic orbit that enters both the bar region and the region of the spirals, but avoids the center of the bar and the regions near the Lagrangian points L_4, L_5. Figure 5 represents an orbit that covers chaotically a large region, including L_4, L_5, but not the center. Finally, Figure 6 shows a chaotic orbit well outside corotation, which does not support the spiral.

Orbits like those of Figures 4 and 5 partially support the bar and/or the spiral outside it. That means that they stay a long time close to the bar and/or the spiral region. They do not support a thin bar or spiral, but they contribute to the density of the bar and the spiral for quite long times (of the order of 10^{10} years; Kaufmann & Contopoulos 1995), thus contributing to the self-consistency of the model.

In a previous paper (Contopoulos et al. 1989) we emphasized the role of gas in supporting a self-consistent spiral from the end of the bar up to the $-4/1$ resonance. We found that a bar plus a self-consistent stellar spiral extending
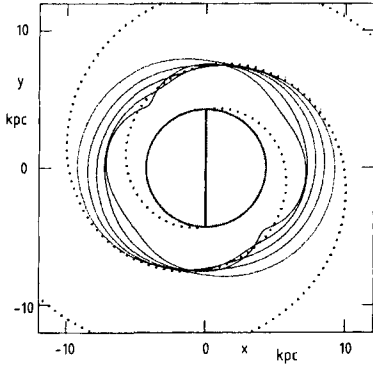
Figure 3. Periodic orbits outside corotation, in the model used by Kaufmann & Contopoulos (1995), supporting the spirals from the $-4/1$ resonance up to the OLR. The imposed spirals emanate from the corotation circle.
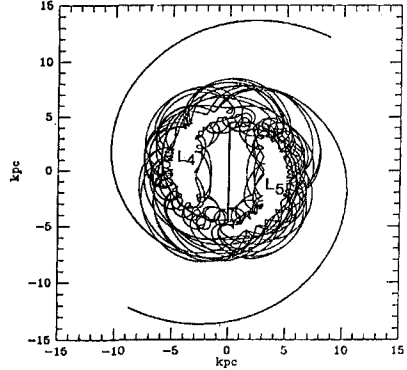
Figure 4. A chaotic orbit supporting both the outer spiral and the bar for a long time. This orbit avoids the center and the Lagrangian points L_4, L_5.

from the $-4/1$ resonance up to the OLR supports a gaseous spiral that joins the bar with the outer stellar spiral. But as many chaotic orbits partly enhance the spiral in this region, it seems that both stars and gas play a role in self-consistent barred galaxies with spirals.

The support of the spirals by chaotic stars is long-lived, but not for infinite times. But this is not a serious problem. In fact spiral galaxies should undergo a secular evolution over periods of some 10^9 years, due to torques (Gnedin et al 1995), therefore one cannot expect self-consistent spirals over longer periods.

2. Transition from Order to Chaos

Chaotic orbits appear always in nonintegrable systems near unstable periodic orbits. Large chaotic regions appear when we have interactions between various unstable periodic orbits (interactions of resonances; Rosenbluth et al. 1966, Contopoulos 1966, 1967, Zaslavskii & Chirikov 1972, Chirikov 1979).

There are three main mechanisms that introduce a large degree of chaos by generating a large number of interacting unstable periodic orbits.

a) Infinite bifurcations (Feigenbaum 1978, Coullet & Tresser 1978, Benettin et al. 1980).
b) Infinite gaps (Contopoulos 1983a) and
c) Infinite spirals (Pinotsis 1991).
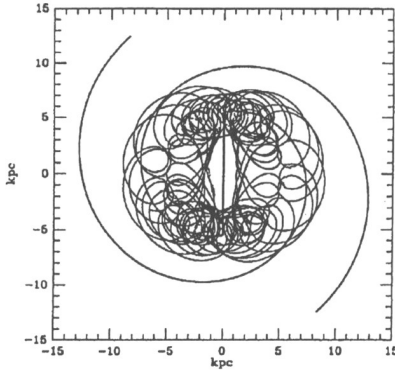
Figure 5.   A chaotic orbit covering L_4, L_5 but not the center. This orbit slightly supports the spiral.
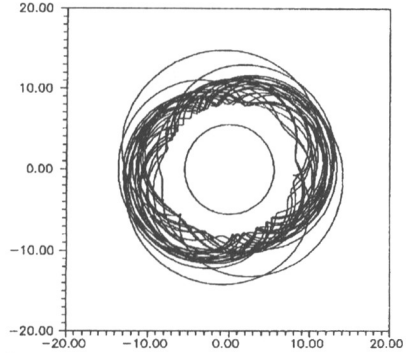
Figure 6.   A chaotic orbit well outside corotation, which does not support the spiral.

(a) Infinite bifurcations.

An example of infinite bifurcation is shown in Figure 7. This case deals with bifurcations from the central family x_1 outside corotation. While the Jacobi constant h increases, the orbits x_1 approach corotation. At a certain value $h = h_1$ the family x_1 becomes unstable, and a family of equal period $(-1/1)$ is generated. When this family becomes unstable, at $h = h_2$, a stable double period family $(-2/2)$ is generated. This, in turn, generates a family $-4/4$, then $-8/8$ etc. After infinite bifurcations, beyond a certain value $h = h_\infty$, we have infinite unstable families of periodic orbits, that introduce a large degree of chaos.

This mechanism is the conservative counterpart of the mechanism discovered by Feigenbaum (1978) and Coullet & Tresser (1978) for dissipative systems. It was first found by Benettin et al. (1980) and its main feature is that the ratio of successive intervals between bifurcations tends to a universal number

$$\frac{h_n - h_{n-1}}{h_{n+1} - h_n} = \delta \to 8.72, \tag{2}$$

which is the conservative counterpart of the dissipative universal bifurcation ratio $\delta = 4.67$.

(b) Infinite gaps.
When we have resonances of the form

$$\frac{\kappa}{\Omega - \Omega_s} = \frac{n}{1} \tag{3}$$

in the axisymmetric background potential V_o (where $\Omega - \Omega_s$ is the angular velocity in the rotating frame and κ the "epicyclic frequency") we have bifurcations
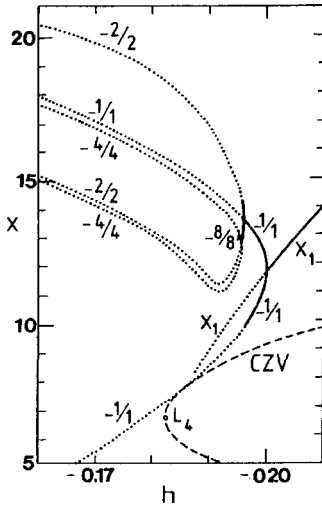
Figure 7. Infinite period doubling bifurcations from the family x_1 outside corotation. The first bifurcation gives an equal period family $(-1/1)$, and this gives infinite period doubling bifurcations. The bifurcation ratio is $\delta = 8.72$.
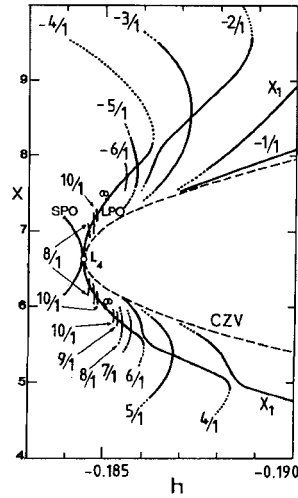
Figure 8. Infinite gaps along the characteristic x_1 (near the resonances 4/1, 6/1,...) appear both inside and outside corotation. These gaps accumulate at the points ∞. Another infinity of gaps appears between ∞ and L_4 along the long period family LPO (at the resonances 8/1,9/1,10/1,...). SPO marks the short period orbits.

of resonant families of periodic orbits from the "central" family x_1 of circular orbits. The introduction of a perturbation εV_1 produces gaps instead of bifurcations if n=even. On the other hand if n=odd we have odd bifurcations followed by small intervals of instability of the family x_1.

The theory of these gaps and instabilities has been developed elsewhere (Contopoulos 1983a). The gaps are larger for smaller n and for larger perturbations ε.

When $\varepsilon = 0$ there is an infinity of bifurcations as h tends to $h(L_4)$. But for $\varepsilon \neq 0$ there is an infinity of gaps terminating at a particular value $h_{\varepsilon\infty}$ (Figure 8).

Between $h_{\varepsilon\infty}$ and $h(L_4)$ there are also infinite gaps between successive parts of the family of long period orbits (LPO). When the perturbation ε is small one has the impression that there is a continuous family of LPO's, which is a continuation of the family x_1 of almost circular orbits, beyond $h_{\varepsilon\infty}$. However the long period family is split into an infinity of families that are generated by bifurcations at particular points of the short period family (SPO in Figure 8) and terminate again at the short period family. These bifurcations are called "branches" in the case of the restricted three body problem (Deprit & Henrard

1968). The topology of the branches in the galactic case has been discussed in detail in a previous paper (Contopoulos 1983b). The gaps between branches increase as the perturbation increases. Most of these orbits are unstable, and for large ε only very small intervals of stability appear, and no impression of continuity of the so-called long period "family" appears.

All the gaps, both for $h < h_{\varepsilon\infty}$ and for $h(L_4) > h > h_{\varepsilon\infty}$, introduce new unstable periodic families. In this way an infinity of unstable families of periodic orbits is generated in the large neighborhood of corotation. Outside corotation we have a similar infinity of gaps and unstable periodic families. All these families contribute to the appearance of chaos in a region around corotation, which becomes larger as the perturbation increases.

(c) Infinite spirals.

If the perturbation ε is large enough, the Lagrangian points L_4, L_5 become unstable. In this case the characteristic of the short period orbits, which has a large stable part, cannot reach L_4. Then most branches, bifurcating from the short period family, form spirals around points having a Jacobi constant equal to that of L_4. Such spirals were derived by Pinotsis (1991) and they generalize the 5 spiral families found by Strömgren (1924) in the restricted three-body problem. A detailed description of these spirals in the galactic case was given in a previous paper (Contopoulos 1988). The main result is the following. When L_4, L_5 are unstable there is an infinity of spirals formed by higher order periodic orbits. As the perturbation ε increases, more spirals are formed by lower and lower order orbits, until the short period orbits themselves generate a spiral.

The orbits belonging to these spiral characteristics form spirals around a Lagrangian point (L_4 or L_5). Such orbits are mostly unstable with only extremely small intervals of stability at the minima and maxima h of every turn of a spiral. Thus we have an infinity of unstable orbits that contribute to the formation of a large chaotic region near corotation.

3.   Spectra of Stretching Numbers

The main characteristic of chaos is the sensitive dependence on initial conditions. This dependence is characterized by a positive maximal Lyapunov Characteristic Number (LCN). On the other hand if an orbit has zero LCN it is ordered.

The maximal Lyapunov characteristic number is defined as the limit

$$LCN = \lim_{t \to \infty} \frac{\ln | \frac{\xi}{\xi_o} |}{t} \qquad (4)$$

where ξ is the deviation between two adjacent orbits at time t, when the initial deviation is ξ_o.

In practice the value

$$\chi = \frac{\ln | \frac{\xi}{\xi_o} |}{t} \qquad (5)$$

approaches a limit only after a very long time, which, in the case of galactic models, is much longer than the age of the Universe. Thus several authors

(Fujisaka 1983, Grassberger et al. 1988, Udry & Pfenniger 1988, Froeschlé et al 1993, Kandrup & Mahon 1994, Voglis & Contopoulos 1994) have calculated finite time Lyapunov numbers. In fact most information about the system is derived if t is small.

In the case of mappings the shortest possible time is $t = 1$. This case has been discussed by Froeschlé et al. (1993) and by Voglis & Contopoulos (1994). We call the quantity

$$a_i = \ln \mid \frac{\xi_{i+1}}{\xi_i} \mid \qquad (6)$$

(where ξ_i is the deviation of an orbit at step i), a "stretching number" (or "short-time Lyapunov number"). The spectrum of the stretching numbers gives the quantity

$$S(a) = \frac{dN(a)}{N\,da} \qquad (7)$$

(where $\frac{dN}{N}$ is the proportion of values of a in a given interval $(a, a + da)$), as a function of a.

We found (Voglis & Contopoulos 1994) that this spectrum is invariant (a) with respect to the initial point along an orbit, (b) with respect to the initial direction of ξ_o, and (c) with respect to the initial conditions, if they are in the same chaotic domain.

The spectra of ordered and chaotic orbits are quite different but they are both invariant. In Figure 9 we find spectra for the standard map

$$y_{n+1} = y_n + \frac{K}{2\pi} \sin 2\pi x_n$$

$$(mod\ 1) \qquad (8)$$

$$x_{n+1} = x_n + y_{n+1}$$

The initial conditions for the first orbit (Figure 9a) are in the chaotic domain while in the second case (Figure 9b) they belong to an island of stability.

Instead of calculating one orbit for a very long time we may take a combined spectrum of many orbits in the same chaotic domain, calculated for a relatively short time. E.g. the combined spectrum of 10^4 orbits in the chaotic domain, calculated for 100 periods each, is practically identical to the spectrum of one orbit calculated for 10^6 iterations (Figure 9a). However if we combine both ordered and chaotic orbits the spectrum is quite different (Figure 10).

The LCN is the average value of the stretching numbers a when $N \to \infty$, i.e. the LCN is the first moment of the spectrum $S(a)$. However the spectrum gives much more information than the LCN, or the distribution of the consequent on a Poincaré surface of section. In Figure 11 we compare two systems that have the same LCN, namely the standard map (8) for $K = 7$, and the (conservative) Hénon map

$$x_{n+1} = 1 - K'x_n^2 - y_n$$

$$(mod\ 1) \qquad (9)$$

$$y_{n+1} = bx_n$$
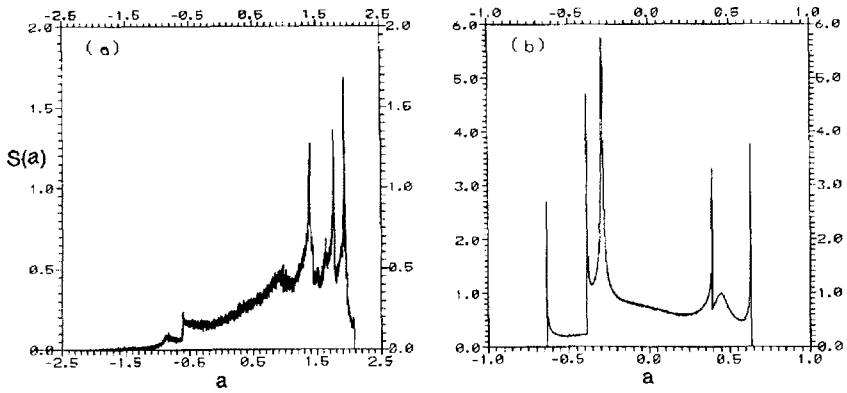
Figure 9.   Invariant Lyapunov spectra of orbits calculated for $N = 10^6$ iterations in the standard map with the same initial conditions $(x_o = 0.1, y_o = 0.5, (dy/dx)_o = 0)$ for $K = 5$ (a) and $K = 0.5$ (b). The first case is chaotic and has a positive LCN, while the second case is ordered and has LCN=0.
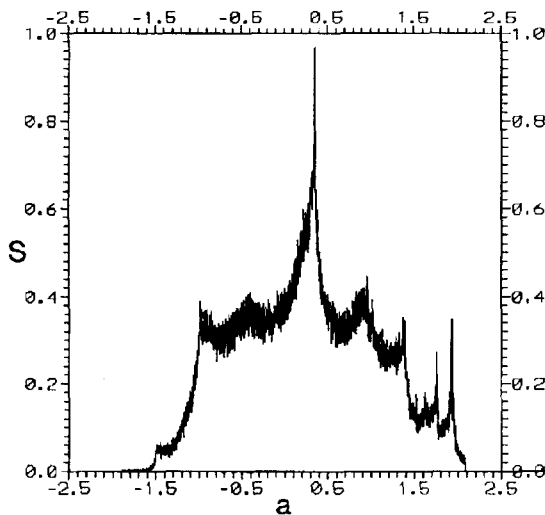
Figure 10.   Combined spectrum of 100×100 orbits, each calculated for N=100 periods (K=5), when part of the orbits are in the ordered domain.

with $b = 1$ and $K' = 5.321$. The LCNs in both cases are equal to $LCN = 1.276$. Figures 11a,c give the distributions of the iterates of the two maps, which look very similar. However the corresponding spectra (Figures 11b, d) are quite different.

4.   Spectra of Galactic Orbits

We can define Lyapunov spectra of conservative dynamical systems by considering the intersections of the orbits by a Poincaré surface of section.

Such is the case of the simple Hamiltonian

$$H = \frac{1}{2}(\dot{x}^2 + \dot{y}^2 + Ax^2 + By^2) - \varepsilon xy^2 = h, \tag{10}$$

that may represent the central parts of a deformed galaxy.

The distribution of the consequents of an orbit in the Poincaré surface of section shows a large chaotic domain with two large islands of stability, plus some very small higher order islands. If we calculate two orbits in the chaotic domain for $N = 10^5$ periods each, we find two spectra that almost coincide (Figure 12) (Contopoulos et al 1995a).

Similar results we find if we calculate the spectra in realistic models of barred galaxies. We have considered a galactic model consisting of a disk, a bar, a spiral and a halo (Kaufmann & Contopoulos 1995). In Figure 13 we have the Lyapunov spectra of two chaotic orbits in this potential. These orbits have the same Jacobi constant but very different initial conditions. The orbits are similar to Figure 4, but different in the details. Nevertheless their spectra are almost identical.

On the other hand the spectrum of a chaotic orbit (Figure 6) for a different Jacobi constant (Figure 14) is different from the above.

5.   Spectra of Dissipative Systems

The Hénon map (9) is dissipative if $b < 1$. In such a case the successive consequents (x_n, y_n) approach an attractor, which may be a point, or a line, or a strange attractor. In each case we have a corresponding invariant spectrum (Voglis & Contopoulos 1994). E.g. in Figure 15a the consequents approach a point attractor. The corresponding spectrum for $N = 10^6$ iterations is given in Figure 15b. This spectrum is invariant, namely the next 10^6 iterations, which are very close to the central point of Figure 15a give the same spectrum as Figure 15b.

Similar results we found for orbits approaching a strange attractor. All these spectra are invariant, as in the conservative case.

We conclude that the spectra of stretching numbers give important information about orbits in galactic systems not only for stars, but also for gas particles, when we have dissipation.
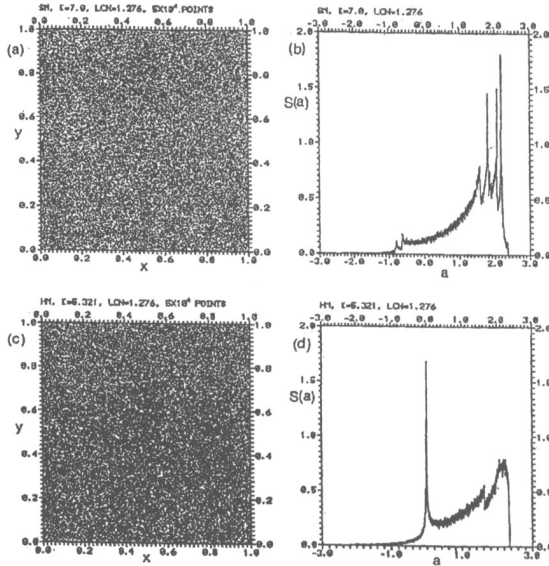
Figure 11.   The distribution of the consequents of two chaotic orbits, one in the standard map (a) and one in the Hénon conservative map (c) look the same, but the corresponding spectra (b and d) are quite different, despite the fact that the Lyapunov numbers are equal.
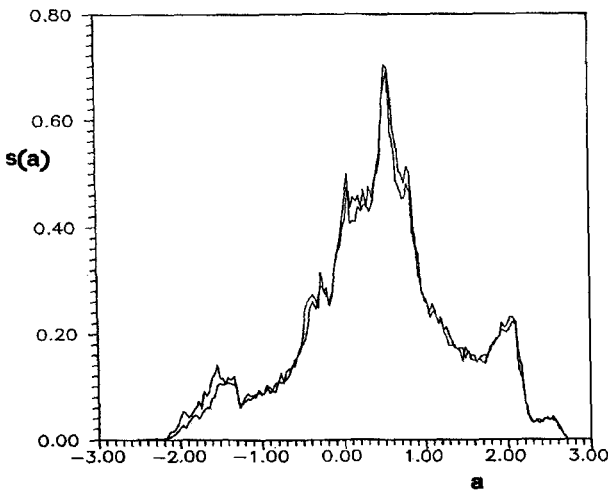
Figure 12.   Spectra of two chaotic orbits of the Hamiltonian (10).
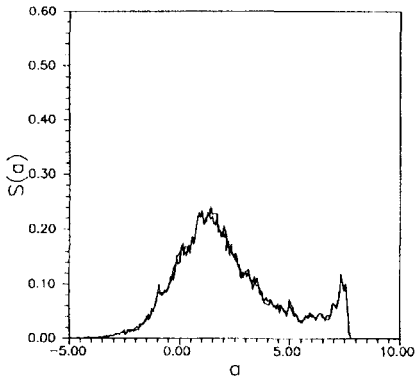
Figure 13. Spectra of two chaotic orbits in a barred spiral model for the same value of the Jacobi constant near corotation.
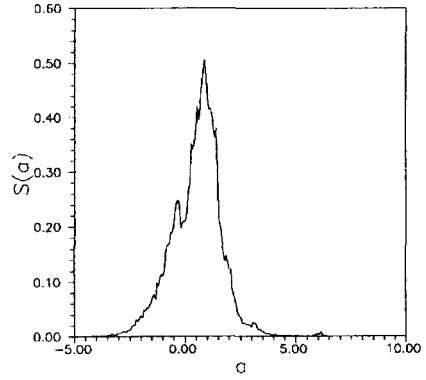
Figure 14. Spectrum of a chaotic orbit in the same model as Figure 13, but with larger Jacobi constant.
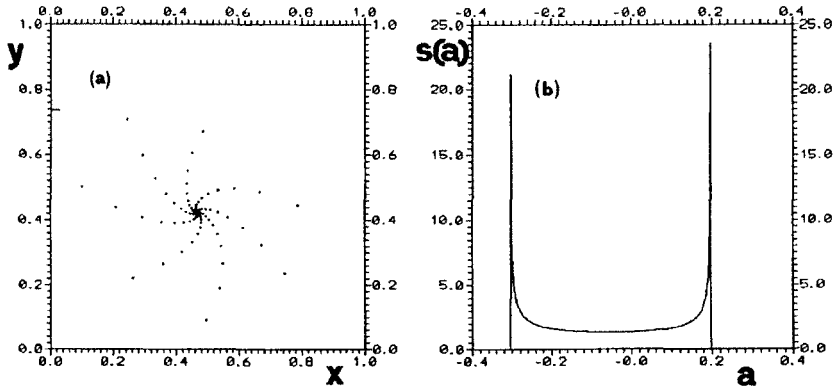
Figure 15. (a) The consequents of an orbit in a dissipative Hénon map (Eq. (9) with K=0.5, b=0.9) with initial conditions ($x_o = 0.1$, $y_o = 0.5$, $(dy/dx)_o = 0$). The orbit approaches a point attractor. (b) The corresponding spectrum for $N = 10^6$ iterations.

6.   Spectra of 3-D Systems

In systems of 3 degrees of freedom we have a new phenomenon for chaotic orbits, namely Arnold diffusion, which does not appear in systems of 2 degrees of freedom. In fact chaotic domains that are separated by KAM tori in 2-D systems are no more separated in 3-D systems.

   This phenomenon has important consequences as regards the spectra of stretching numbers. Namely the spectra look different for a certain interval of time, but after a much longer time they tend to become identical (Contopoulos et al 1995b).

   A Poincaré surface of section for a time-independent 3-D Hamiltonian system (with fixed energy) is 4-dimensional. We have studied a simple 4-D map that has the basic properties of a map derived from a 3-D Hamiltonian, namely it is symplectic:

$$y_1' = y_1 + \frac{K}{2\pi} \sin 2\pi x_1 - \frac{\beta}{\pi} \sin 2\pi (x_2 - x_1)$$

$$x_1' = x_1 + y_1'$$

$$(mod\ 1) \qquad (11)$$

$$y_2' = y_2 + \frac{K}{2\pi} \sin 2\pi x_2 - \frac{\beta}{\pi} \sin 2\pi (x_1 - x_2)$$

$$x_2' = x_2 + y_2'$$

   This map consists of two coupled standard maps. For $\beta = 0$ the maps on the planes (x_1, y_1) and (x_2, y_2) are independent. But as soon as β is different from zero the two maps are coupled and one influences the other.

   In Figure 16 we have the distribution of the consequents on the plane (x_1, y_1) for a small value of β ($\beta = 0.1$). The thick lines represent invariant curves for the standard map when $\beta = 0$. But with $\beta = 0.1$ the consequents have some spreading indicating a small degree of chaos.

   When $\beta = 0.30$ the chaotic regions increase, but still they are not spread over the whole available area (x_1, y_1) for a quite long time (Figure 17). But when β changes a little further ($\beta = 0.30513$, Figure 18) after some time the consequents escape from the confined region and fill the whole space (x_1, y_1). For still larger β (e.g. $\beta = 0.31$) the spreading of the consequents is completely uniform over the whole space (x_1, y_1).

   The corresponding spectra of stretching numbers are given in Figure 19. The spectrum for $\beta = 0.30$ (a) is around $a = 0$, and the Lyapunov characteristic number (LCN) is almost zero. The spectrum for $\beta = 0.30513$ (b) has a large extension towards positive values of a and its LCN is definitely positive. Finally the spectrum for $\beta = 0.31$ (c) has an even larger LCN. This spectrum is truly invariant, i.e. it does not change in time, or with different initial conditions in the chaotic domain.

   The spectrum for $\beta = 0.30513$ is a transient one. As time increases it approaches the form of the spectrum for $\beta = 0.31$.

   The diffusion time increases considerably as β decreases. It is $T = 10^5$ periods for $\beta = 0.30513$, while it is 2×10^7 periods for $\beta = 0.30512$. For
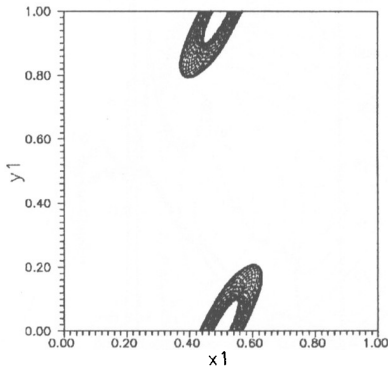
Figure 16. The distribution of the consequents of the map (11) with $\beta = 0.1$ and initial conditions ($x_1 = 0.55$, $y_1 = 0.1$, $x_2 = 0.62$, $y_2 = 0.2$).
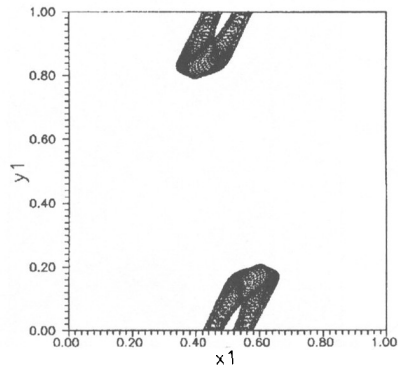
Figure 17. The same as in Figure 16 for $\beta = 0.30$.

$\beta = 0.30$ it seems that the diffusion time is so large that it will never be possible to find it by numerical calculations. Thus we may say that the spectrum for $\beta = 0.30$ in Figure 19 is invariant for all practical purposes.

It is important that only for a rather small range of values of β we have transient spectra over a relatively long time.

We conclude that an important characteristic of Arnold diffusion is a transient spectrum. But the time scale of Arnold diffusion for most cases is either short, or exceedingly long, and thus irrelevant for applications. In particular in most cases of galactic dynamics this diffusion is either indistinguishable from the usual diffusion through cantori, that we encounter in systems of 2 degrees of freedom, or so exceedingly slow that it can be ignored.

7. Very Short-Time Spectra

In the case of Hamiltonian systems we can take the short-time Lyapunov numbers for a time interval much shorter than one period. One of the shortest time intervals is the integration step Δt.

If Δt is small the stretching number [Eq. (6)] becomes proportional to Δt (Smith & Contopoulos 1995). For this reason a better definition of the stretching number is

$$\bar{a}_i = \frac{1}{\Delta t} \ln | \frac{\xi_{i+1}}{\xi_i} | \tag{12}$$

and this value is independent of Δt.

We have found the short-time Lyapunov characteristic numbers in the case of a Hamiltonian depending periodically on the time. This refers to an oscillating
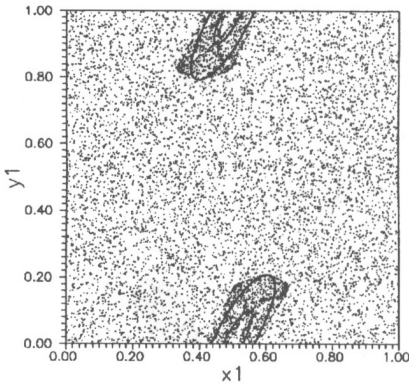
Figure 18.   The same as in Figure 16 for $\beta = 0.31$.
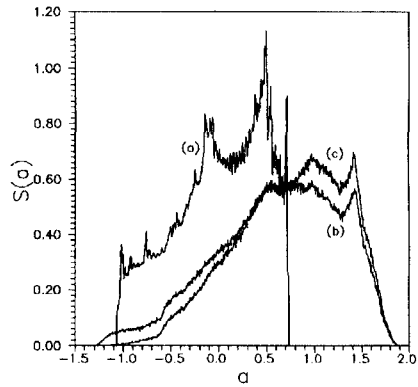
Figure 19.   Spectra of stretching numbers for (a) $\beta = 0.30$, (b) 0.30513, (c) 0.31 and $N = 10^6$.

model of a galaxy, that represents the outcome of a spherical collapse, as found empirically by Miller & Smith (1994).

If we plot the values of R and $\dot{R}$ at every period T we find a Poincaré surface of section (Figure 20) that contains both ordered and chaotic regions.

The spectrum of the stretching numbers for a step $\Delta t = 0.125$ is given in Figure 21. The initial conditions are in the small chaotic domain near $R = 18$. Another spectrum with different initial conditions in the same chaotic domain is indistinguishable from the above. However the spectrum of an ordered orbit, or of a chaotic orbit in another chaotic domain is different.

In order to find the spectra of stretching numbers for a longer time $\Delta T = m\Delta t$ we write

$$\bar{\bar{a}}_i = \frac{1}{\Delta T} \ln \frac{\xi_{i+m}}{\xi_i} = \frac{1}{\Delta T}[\ln \frac{\xi_{i+m}}{\xi_{i+m-1}} + ... + \ln \frac{\xi_{i+1}}{\xi_i}] =$$

$$\frac{1}{m} \sum_{j=i}^{i+m-1} \bar{a}_j. \tag{13}$$

The corresponding spectrum $S(\bar{\bar{a}})$ can be derived directly from the data stored for the curve $S(\bar{a})$.

8.   Conclusions

We studied the transition from ordered to chaotic orbits in barred galaxies. Some chaos appears always near unstable periodic orbits (resonant orbits) in nonintegrable dynamical systems. But large chaos appears through the interaction of many resonances. There are three basic mechanisms that introduce such resonance interactions:
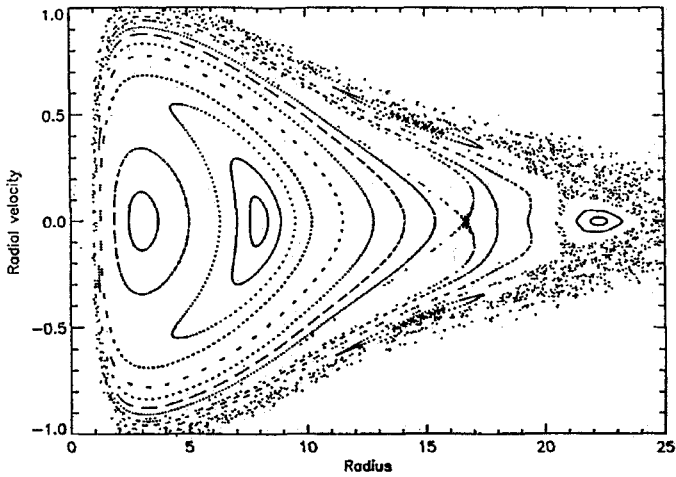
Figure 20.   The Poincaré surface of section $t = mT$ for the model of Smith & Contopoulos (1995). The 1:1 resonance is at $R = 8$, and the 2:1 resonance at $R = 16.7$.
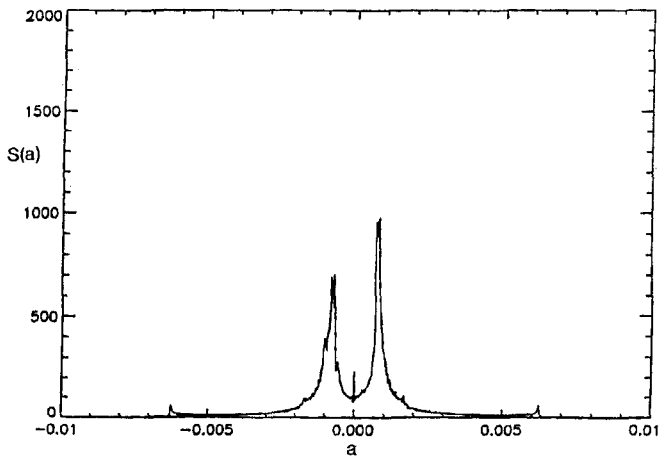
Figure 21.   Spectra of stretching numbers of two chaotic orbits with initial conditions in the resonance region 2/1, for $N = 10^6$ periods each and step $\Delta T = \Delta t = 0.125$. The two spectra are indistinguishable.

(1) Infinite period doubling bifurcations,
(2) Infinite gaps in the characteristics, and
(3) Infinite spiral characteristics (when L_4, L_5 become unstable).

All these mechanisms appear in the larger neighborhood of corotation.

Chaotic orbits near corotation play a role in constructing self-consistent models of barred galaxies, because they partially support the bar and the spiral for quite long times (of order 10^{10} years). On the other hand there are chaotic orbits beyond corotation that do not support the spiral.

A new method to study chaotic orbits is by calculating the spectra of their stretching numbers, i.e. the distribution of their short-time Lyapunov numbers.

We have considered two short times.

(a) $t = 1$ and
(b) $t =$ the integration step $\Delta t \ll 1$.

The first case applies to maps, including the maps on a Poincaré surface of section of continuous systems, while the second case applies only to continuous systems.

The spectra, calculated for a rather large number of iterations N, are invariant: (1) with respect to the initial position along an orbit, (2) with respect to the direction of the initial deviation ξ_o from a given orbit, and (3) with respect to initial conditions in the same (connected) chaotic domain.

The last property allows one to find the invariant spectrum of a chaotic domain of a galaxy by calculating many nearby orbits over relatively short times. E.g. instead of calculating an orbit for 10^6 periods, one can calculate 10^4 orbits for 100 periods (about one Hubble time) and superimpose their spectra. One has only to be careful not to mix together ordered and chaotic orbits.

The usual Lyapunov characteristic number is the first moment of the spectrum.

The spectra of the stretching numbers give much more information about a system than the Lyapunov characteristic number alone. We give an example of two chaotic systems that have the same LCN, and fill equally densely the whole chaotic domain, but still have very different spectra.

The use of times much shorter than $t = 1$ is possible in continuous systems. The spectrum derived for short times Δt is independent of the size of Δt if Δt is sufficiently small. This means that we do not find more information by reducing the size Δt further. The spectrum for a longer step $\Delta T = m\Delta t$ can be derived from the spectrum for Δt, but not vice versa.

We have found invariant spectra in the following cases:
(a) 2-D conservative maps
(b) 2-D Hamiltonian systems. In particular we found spectra for a simple model of the central regions of a deformed galaxy and for a realistic model of a barred galaxy, composed of a disk, a bar, a spiral and a halo.
(c) Dissipative systems.
(d) 3-D Hamiltonian systems, represented by 4-D symplectic maps. In this case we found the importance of Arnold diffusion in various cases.

(e) Time-dependent Hamiltonians. In particular we studied a spherical galaxy undergoing periodic oscillations.

We conclude that the spectra of stretching numbers (or spectra of short-time Lyapunov numbers) are very important in finding the basic characteristics of the orbits of a dynamical system, and in particular of the chaotic orbits.

References

Benettin, G., Cercignani, C., Galgani, L., & Giorgilli, A. 1980, Lett. Nuovo Cim., 29, 1

Chirikov, B.V. 1979, Phys. Rep., 52, 263

Contopoulos, G. 1966, in Les Nouvelles Méthodes de la Dynamique Stellaire, F. Nahon & Hénon, M., Paris: CNRS

Contopoulos, G. 1967, Bull. Astron., 2, Fasc. 1, 223

Contopoulos, G. 1980, A&A, 81, 198

Contopoulos, G. 1983a, Physica, 8D, 142

Contopoulos, G. 1983b, Cel. Mech., 31, 193

Contopoulos, G. 1988, Cel. Mech., 43, 147

Contopoulos, G., Gottesman, S. T., Hunter, J. H., & England, M. N. 1989, ApJ, 343, 608

Contopoulos, G. & Grosbol, P. 1989, A&ARev., 1, 261

Contopoulos, G., Kandrup, H., & Kaufmann, D. 1993, Physica D, 64, 310

Contopoulos, G., Grousousakou, E., & Voglis, N. 1995a, A&A, in press

Contopoulos, G., Voglis, N., Efthymiopoulos, C., & Grousousakou, E. 1995b, in Waves in Astrophysics, J. Hunter & R. Wilson, Ann. N. Y. Acad. Sci., in press

Coullet, P. & Tresser, C. 1978, J. de Physique, 39, C5

Deprit, A. & Henrard, J. 1968, Adv. Astron. Astrophys., 6, 1

Feigenbaum, M. 1978, J. Stat. Phys., 19, 25

Froeschlé, C., Froeschlé, C., & Lohinger, E. 1993, Celest. Mech. Dyn. Astron., 56, 307

Fujisaka, H. 1983, Prog. Theor. Phys., 70, 1264

Gnedin, O. Y., Goodman, J., & Frei, Z. 1995, Princeton Obs. preprint

Grassberger, P., Badii, R., & Politi, A. 1988, Stat. Phys., 51, 135

Kandrup, H. E. & Mahon, M. E.: 1994, in Three-Dimensional Systems, H. E. Kandrup, S. Gottesman, & J. Ipser, Ann. N. Y. Acad. Sci., 751, 93

Kaufmann, D. & Contopoulos, G. 1995, A&A, in press

Miller, R. H. & Smith, B. F. 1994, Cel. Mech. Dyn. Astron., 59, 161

Pinotsis, A. 1991, in Long Term Behaviour of Natural and Artificial N-Body Systems, A. Roy, Dordrecht: Kluwer, 465

Rosenbluth, M. N., Sagdeev, R. A., Taylor, J. B., & Zaslavskii, M. 1966, Nucl. Fusion, 6, 217

Smith, H. & Contopoulos, G. 1995, in Waves in Astrophysics, J. Hunter & R. Wilson, Ann. N. Y. Acad. Sci., in press

Strömgren, E. 1924, Copenhagen Obs. Publ. 47

Udry, S. & Pfenniger, D. 1988, A&A, 198, 135

Voglis, N. & Contopoulos, G. 1994, J. Phys., A 27, 5357

Zaslavskii, G. M. & Chirikov, B. V. 1972, Sov. Phys. Uspekhi, 14, 549

Discussion

B. Elmegreen: Where can we have shocks due to the resonances?

G. Contopoulos: In Figure 1 of my paper we see where the orbits of two families intersect (families x_1 and 4/1), or the orbits of one family develop loops (e.g. family x_1). At such intersection points we expect shocks. But such shocks appear in certain intervals of radii, and not only at one radius.

Anonymous: Can you comment on the fraction of time that a chaotic orbit can support non-axisymmetric structure? Is there a practical way to determine this?

G. Contopoulos: The only way is by numerical calculations of typical orbits. In some cases we found partial support of the bar and of the spiral for 10^{10} years.

P. Teuben: How did the time varying potential from the Miller and Smith bar result in such nice invariant curves?

G. Contopoulos: In a generic nonintegrable potential varying periodically in time one finds both ordered regions with closed invariant curves, and chaotic regions.

J. Sellwood: Could the properties of stretching numbers be used to devise a technique for distinguishing regular from chaotic orbits that is more efficient than calculation of Lyapunov numbers?

G. Contopoulos: The fastest way to distinguish between regular and chaotic orbits is by calculating the distribution of a number of consequents. The stretching numbers give much more information than simply whether an orbit is regular or chaotic.

E. Athanassoula: How does your method compare to Laskar's frequency analysis method?

G. Contopoulos: We study the stretching numbers along an orbit, while Laskar analyzes the rotation angles. But the distribution of the rotation angles also gives a spectrum, in the same way as the distribution of stretching numbers.